Probing the Transmembrane Structure and Dynamics of Microsomal NADPH-cytochrome P450 oxidoreductase by Solid-State NMR

Rui Huang,[†] Kazutoshi Yamamoto,[†] Meng Zhang,[†] Nataliya Popovych,[†] Ivan Hung,[¶] Sang-Choul Im,[‡§] Zhehong Gan,[¶] Lucy Waskell,[‡§] and Ayyalusamy Ramamoorthy[†*]

[†]Biophysics and Department of Chemistry, University of Michigan, Ann Arbor, Michigan; [‡]Department of Anesthesiology, University of Michigan, Ann Arbor, Michigan; [§]Veterans Administration Medical Center, Ann Arbor, Michigan; and [¶]National High Magnetic Field Lab, Tallahassee, Florida

ABSTRACT NADPH-cytochrome P450 oxidoreductase (CYPOR) is an essential redox partner of the cytochrome P450 (cyt P450) superfamily of metabolic enzymes. In the endoplasmic reticulum of liver cells, such enzymes metabolize ~75% of the pharmaceuticals in use today. It is known that the transmembrane domain of CYPOR plays a crucial role in aiding the formation of a complex between CYPOR and cyt P450. Here we present the transmembrane structure, topology, and dynamics of the FMN binding domain of CYPOR in a native membrane-like environment. Our solid-state NMR results reveal that the N-terminal transmembrane domain of CYPOR adopts an α-helical conformation in the lipid membrane environment. Most notably, we also show that the transmembrane helix is tilted ~13° from the lipid bilayer normal, and exhibits motions on a submillisecond timescale including rotational diffusion of the whole helix and fluctuation of the helical director axis. The approaches and the information reported in this study would enable further investigations on the structure and dynamics of the full-length NADPH-cytochrome P450 oxidoreductase and its interaction with other membrane proteins in a membrane environment.

INTRODUCTION

Approximately 75% of the pharmaceuticals in use today are metabolized by a group of heme-containing monooxygenases known as the cytochrome P450 (cyt P450) superfamily. These enzymes are responsible for the metabolism of a great number of endogenous compounds including vitamins, steroids, and hormones, as well as exogenous compounds including environmental toxins and drugs. Cyt P450s catalyze a variety of chemical transformations by activating stable carbon-hydrogen bonds of alkanes using oxygen and electrons from their redox partners. Due to the strong and versatile oxidizing capability of cyt P450, they are referred to as "mother nature's blowtorch".

NADPH-cytochrome P450 oxidoreductase (CYPOR) is an essential redox partner of microsomal cyt P450s, which shuttles electrons from NADPH to cyt P450s. Additionally, CYPOR plays an indispensable role in the development of high-level organisms; it is also able to reduce cytochrome *c*, cytochrome b_5, and heme oxygenase as well as a variety of therapeutic prodrugs (1–5). CYPOR is a multidomain membrane protein composed of a soluble 70-kDa carboxyl terminal catalytic domain, a 5-kDa amino terminal transmembrane segment, and a 2-kDa linker connecting these two domains. The soluble domain of CYPOR, whose structure has been characterized by x-ray crystallography (6,7), can be further divided into the FAD/NADPH binding domain and the FMN binding domain. The structures of the transmembrane domain and the linker region remain unidentified. An electron transfer pathway originates from NADPH, which transfers a hydride ion to the cofactor FAD, which proceeds to donate the electrons to the cofactor FMN. The FMN binding domain is the ultimate donor of electrons to cyt P450s and other protein acceptors.

It has long been postulated that the transmembrane domain of CYPOR plays a vital role in aiding the electron transfer between CYPOR and cyt P450 (8–10). Lacking the transmembrane anchor, CYPOR is still able to reduce cytochrome *c* and other artificial acceptors, but is impaired in transferring electrons to cyt P450 (6). Truncation of the N-terminal segment leads to a severe decrease/prohibition of substrate turnover in a reconstituted cyt P450 system (8). However, the mechanism for how the transmembrane domain affects the cyt P450/CYPOR interaction and catalysis remains under debate. It is generally believed that the transmembrane domain of CYPOR anchors the enzyme on the surface of the membrane, thereby constraining the diffusion of the catalytic soluble domain and mediating the CYPOR/cyt P450 interaction so as to achieve its proper orientation (9). Other hypotheses have been raised that the N-terminal transmembrane domain of CYPOR in its free form can alter the dynamics of diffusive reduced oxygen species, thus affecting the substrate catalysis (8). A complete understanding of the physiological function of the transmembrane domain requires a complete characterization of its structure and dynamics in a lipid membrane environment. Despite postulations about its secondary structure (10–13), a high-resolution structure of the transmembrane domain has not been revealed experimentally, even though the first structure of

Submitted November 27, 2013, and accepted for publication March 19, 2014.

*Correspondence: ramamoor@umich.edu

Editor: Heiko Heerklotz.

0006-3495/14/05/2126/8 $2.00

http://dx.doi.org/10.1016/j.bpj.2014.03.051

the soluble domain of rat CYPOR was determined in 1997 by x-ray crystallography (6). The major difficulty lies in the hydrophobicity and mobility of the transmembrane domain, preventing it from crystallization with the soluble domain.

Solid-state nuclear magnetic resonance (NMR) spectroscopy is a powerful approach to probe the high-resolution structure and dynamics of insoluble, noncrystalline, or amorphous biomolecules such as membrane proteins. Here, we present the biological expression and purification of the N-terminal FMN binding domain of CYPOR, which includes the transmembrane domain and the linker region. To our knowledge, this also constitutes the first solid-state NMR investigation on its structural and dynamic features in a native membrane-like environment.

MATERIALS AND METHODS

Expression and purification of a uniformly ^{15}N labeled FMN binding domain of rat NADPH-cytochrome P450 oxidoreductase (CYPOR)

Membrane-bound FMN binding domain (MFBD) was expressed and purified from *E. coli* C41 using a pSC-CPR plasmid (14); the amino-acid sequence of MFBD is given in the Supporting Material. After adaptation of cells in 100 mL modified LB medium containing 1% (w/v) NaCl, 1% (w/v) yeast extract, 1% (w/v) tryptone, 0.2% (w/v) glucose, 5.3 nM riboflavin, pH 7.2, cells were cultured in M9 minimal medium containing 40 mM Na_2HPO_4, 20 mM KH_2PO_4, 8.5 mM NaCl, 18 mM $^{15}NH_4Cl$, 1 mM $MgSO_4$, 1 μM $CaCl_2$, 16 nM riboflavin, and 0.4% (w/v) glucose. Expression of MFBD was induced by 0.4 mM IPTG when the cell density reached $A_{600} = 0.7 \sim 0.8$ optical density. After induction, the culture was incubated for 12 h at 30°C, shaken at a speed of 140 rpm, and then harvested by centrifugation. The harvested cells were treated with lysozyme (30 μg per mL of cell suspension) followed by sonication. The membrane fraction of cells was solubilized with 0.3% (w/v) Triton X-100 at 4°C. MFBD was purified using DEAE Sepharose anion exchange and hydroxyapatite chromatography. The detergent-solubilized proteins were loaded into DEAE column and washed with 0.2 M NaCl. MFBD was eluted by a linear salt gradient elution from 0.2 to 0.5 M NaCl. The eluted protein solution was subjected to a hydroxyapatite column to remove the detergents.

The concentration of the oxidized MFBD was determined using extinction coefficient of 12.2 mM^{-1} cm^{-1} at 450 nm (15). The purity of the protein was examined by sodium dodecyl-sulfate polyacrylamide gel electrophoresis (SDS-PAGE), the determination of UV-Vis absorbance, and the use of a Pierce BCA Protein Assay Kit (Thermo Fisher Scientific, Waltham, MA).

Preparation of bicelles

DLPC (1,2-dilauroyl-*sn*-glycero-3-phosphatidylcholine) and DHPC (1,2-dihexanoyl-*sn*-glycero-3-phosphatidylcholine) were purchased from Avanti Polar Lipids (Alabaster, AL). Quantities of 35.95 mg DLPC, 6.55 mg DHPC, and 2.23 mg cholesterol corresponding to a molar ratio of DLPC/DHPC/cholesterol = 4:1:0.4 were cosolubilized in chloroform. Solvent was removed under a stream of N_2 gas to produce a film on the walls of a glass vessel, which was kept in vacuum overnight to remove any residual solvent. A quantity of 21.3 μL of 40 mM potassium phosphate buffer, pH 7.4, with 5% (w/v) glycerol was added to the dry lipid film. The resulting mixture, of extreme viscosity, was homogenized by vortexing, and freeze/heat cycles between 0°C and room temperature for 5–8 times were imposed until the bicelles became transparent and homogeneous. Protein was added in the final step of the preparation.

Addition of 2.5 mg or 92.6 nmol protein in 65 μL of 40 mM potassium phosphate buffer, pH 7.4, with 5% (w/v) glycerol into the bicelle mixture resulted in a protein/DLPC molar ratio of 1:625. The homogeneously mixed sample was packed in a glass tube and used for subsequent NMR experiments. Before NMR measurements, the sample inside the probe was treated with a minimum of three cooling/heating cycles between 7 and 25°C to ensure homogenous alignment of bicelles (16). Hydrogen/deuterium (H/D) exchange experiments were carried out on DLPC/DHPC/cholesterol bicelles containing the membrane-bound FMN binding domain, which were prepared using the protocol described above. The sample was placed under a stream of N_2 gas to partly remove H_2O until the total sample volume was reduced by ~25%. Equivalent amount of the D_2O (i.e., one-fourth of the total sample volume) was added to the sample and mixed until homogenous by vortexing. After 10 cycles of H_2O evaporation/D_2O addition, the sample tube was sealed and transferred to the magnet for subsequent NMR measurements.

NMR experiments

All one-dimensional ^{31}P and ^{15}N NMR spectra were obtained from a 600-MHz NMR spectrometer (Bruker Biosciences, Billerica, MA) using a homebuilt 5-mm electric-field-free flat-coil probe. ^{31}P NMR spectra were obtained using a one-pulse sequence with a recycle delay of 3 s and 25-kHz proton decoupling during ^{31}P signal acquisition. ^{15}N NMR spectra were obtained using refocused-insensitive-nuclei-enhanced-by-polarization transfer (RINEPT) (17,18) and ramped cross-polarization (CP) (19) pulse sequences with a recycle delay of 3.5 s and 55 kHz proton decoupling during ^{15}N signal acquisition.

In the RINEPT experiments, τ-180°-τ delays of 1.3 and 0.65 ms were used before and after a pair of 90° pulses, respectively. In the CP experiments, the contact time was varied from 0.05 to 2 ms. The two-dimensional separated-local-field (SLF) spectrum was obtained on a 720-MHz NMR spectrometer (Agilent) under static conditions using a SAMPI4 sequence with 0.5-ms contact time and 25-kHz small-phase-incremental alternation (SPINAL) decoupling of protons. The two-dimensional spectrum was acquired with 28 t_1 increments, 25-ms acquisition time, 2000 scans, and a 2.5-s recycle delay, resulting in a total experimental time of 39 h. A 5-mm electric-field-free double-resonance static probe (20) was used to prevent sample heating. All NMR experiments were performed at 20°C.

Helical-wheel simulations

A list of resolved peaks from the two-dimensional SLF spectrum of magnetically aligned bicelles containing the protein were extracted as pairs of ^{15}N chemical-shift and ^{15}N-^{1}H dipolar coupling values and arranged to fit the helical wheels by using a homewritten program in which the helical-wheel patterns were predicted by geometrical calculations, as explained in Soong et al. (21).

RESULTS

Magnetic-alignment of bicelles containing MFBD

Bicelles composed of DLPC/DHPC/cholesterol and ^{15}N-labeled membrane-bound FMN binding domain (MFBD) were prepared as described in the Materials and Methods; a schematic illustration of the molecular system under investigation is shown in Fig. 1 *A*. The appearance of a single band on the gel from SDS-PAGE reveals the purity of the protein (Fig. 1 *B*). ^{31}P NMR experiments were performed on bicelles

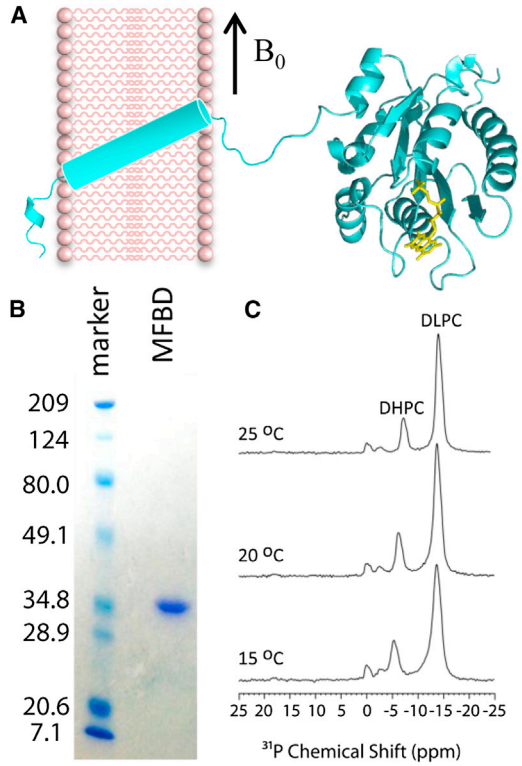

FIGURE 1 (*A*) A schematic of MFBD with its N-terminal transmembrane domain incorporated in lipid bilayers. (*B*) SDS-PAGE gel of MFBD. (*C*) Proton-decoupled ^{31}P chemical-shift spectra of DLPC/DHPC/cholesterol bicelles containing MFBD. Narrow peaks from DLPC and DHPC demonstrate a high degree of alignment of bicelles. Peaks observed at 0 ppm are from phosphorous atoms of the FMN molecule. To see this figure in color, go online.

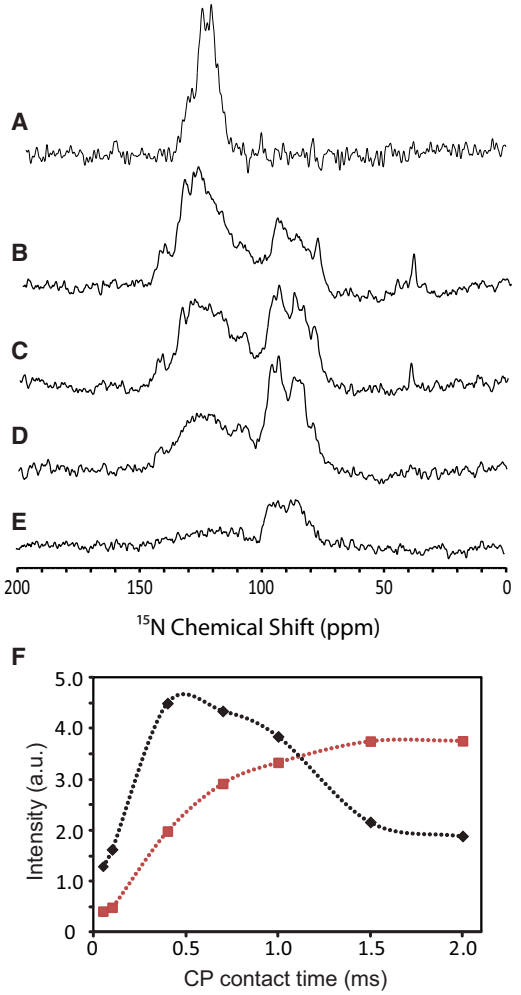

FIGURE 2 ^{15}N NMR spectra of ^{15}N-labeled MFBD incorporated in magnetically aligned bicelles were obtained using RINEPT (*A*) and ramped cross-polarization (CP) with a contact time of 2.0 ms (*B*), 1.0 ms (*C*), 0.4 ms (*D*), and 0.1 ms (*E*). The RINEPT spectrum (*A*) shows spectral intensity only in the 100–140 ppm region, indicating the high mobility of the soluble domain. Resonances in the 70–100-ppm region in the CP spectra (*B–E*) are assigned to the immobile transmembrane domain. Buildup curves (*F*) were measured for resonances at 93.5 ppm (*black*) and 128.4 ppm (*red*) representing the two chemical-shift regions corresponding to two different domains of the protein. To see this figure in color, go online.

under various conditions to determine the magnetic-alignment of the sample. ^{31}P NMR spectra shown in Fig. 1 *C* contain two major peaks: a high-field peak (~−13 ppm) from the lipid DLPC and a low-field peak (~−5 ppm) from the detergent DHPC. The peak positions for DHPC and DLPC confirm the magnetic-alignment of bicelles with the lipid bilayer normal perpendicular to the external magnetic field B_0 (22,23). ^{15}N NMR experiments were also carried out to confirm the alignment of the protein incorporated in bicelles, as explained below.

^{15}N NMR experiments to determine the topology and dynamics of MFBD

One-dimensional ^{15}N NMR spectra of magnetically aligned bicelles containing ^{15}N-labeled MFBD were recorded using ^{1}H-^{15}N polarization transfer schemes, such as RINEPT and CP and with various cross-polarization contact times to achieve optimal intensities of ^{15}N resonances:

1. The absence of chemical shift anisotropic powder pattern in the ^{15}N spectra shown in Fig. 2, *A–E* confirms the alignment of the protein incorporated in bicelles.
2. The ^{15}N spectra exhibit distinct profiles that reveal the topology and dynamics of the protein as explained below.

In the series of ^{15}N CP spectra (Fig. 2, *B–E*), the resonances distribute in two different chemical shift regions: 70–100 and 100–140 ppm. The overall peak intensities in these two regions change when the CP contact time is varied to control the extent of magnetization transfer from ^{1}H to ^{15}N nuclei. The appearance of peaks in the 70–100 ppm region even for a short CP contact time (Fig. 2 *E*) indicates that these signals arise from immobile residues of the protein, most likely from the transmembrane domain of MFBD; this is further confirmed by H/D exchange experiments, as described below in Fig. 3. Use of longer CP

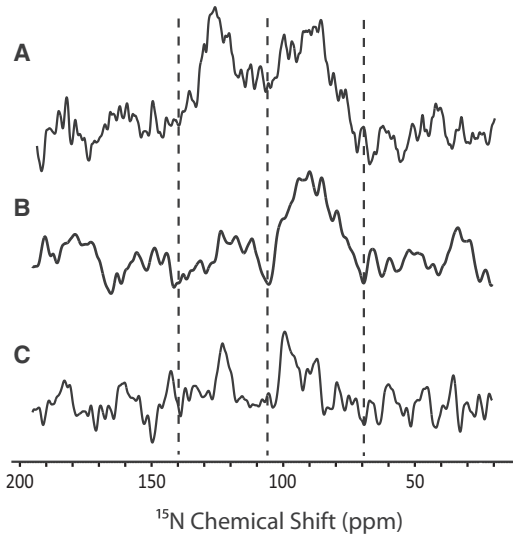

FIGURE 3 Hydrogen/deuterium exchange spectra of ^{15}N-labeled MFBD incorporated in magnetically aligned bicelles. ^{15}N NMR spectra were obtained using ramped cross-polarization with a contact time of 0.5 ms before H/D exchange (*A*), and 5 h (*B*), and 17 h (*C*) after H/D exchange.

contact times (Fig. 2, *B–D*) allows magnetization transfer not only to the rigid transmembrane region (70–100 ppm) but also to some relatively mobile residues in the soluble domain of the protein, giving rise to signals in the 100–140 ppm region.

An RINEPT experiment was employed to detect the mobile region of the protein (11–13). In the RINEPT spectrum (Fig. 2 *A*), peaks in the 70–100 ppm region arising from the transmembrane domain are significantly suppressed while most peaks from the soluble domain region (100–140 ppm) are present. This is due to the fast spin-spin relaxation of the residues in the transmembrane domain of MFBD during the evolution as well as refocusing delays in the RINEPT pulse sequence, which were caused by strong ^{1}H-^{15}N and ^{1}H-^{1}H dipolar couplings. An increase in the CP contact time (Fig. 2, *B* and *C*) increases the intensity of peaks arising from the soluble domain of the protein (100–140 ppm) but decreases that from the transmembrane domain (70–100 ppm) due to $T_{1\rho}$ relaxation. This observation also indicates that motions of residues in the transmembrane domain are more restricted than the residues in the soluble domain.

To confirm the above-mentioned assignment of peaks in the ^{15}N NMR spectra to the soluble and transmembrane domains of the MFBD protein, we carried out NMR experiments utilizing the H/D exchange to suppress the ^{15}N signals from the solvent-accessible residues of the protein. As shown in Fig. 3, before H/D exchange, resonances of MFBD appear in 70–100 and 100–140-ppm chemical-shift regions of the ^{15}N spectrum (Fig. 3 *A*). After 5 h of H/D exchange, the ^{15}N spectrum shows resonances only in the 70–100-ppm chemical-shift region (Fig. 3 *B*). This experimental observation suggests that these resonances in the 70–100-ppm region arise from solvent-inaccessible residues of the protein, which are located in the transmembrane domain of the protein that is embedded in the hydrophobic region of the lipid bilayer. However, the resonances in the 100–140-ppm chemical-shift region show a drastic intensity reduction due to H/D exchange (Fig. 3 *B*), implying that they correspond to the residues from the soluble domain of the protein that are accessible to the solvent. These results confirmed the above-mentioned assignment of the two distinct chemical-shift regions of the one-dimensional ^{15}N NMR spectra in Fig. 2. This spectral assignment approach is similar to that utilized in our previous studies on a membrane-bound cytochrome b_5 (24,25). A longer time-exposure of the MFBD to D_2O leads to further reduction of ^{15}N signals in both 100–140 and 70–100-ppm regions, as shown in Fig. 3 *C*.

Dynamics are crucial for the physiological function of a protein and for protein-protein interactions. Parameters characterizing protein dynamics can be extracted from CP buildup curves that report the rates of magnetization transfer from protons to ^{15}N nuclei. The buildup rate of peak intensities measured at 93.5 ppm (corresponding to the transmembrane domain) and 128.4 ppm (corresponding to the soluble domain) are different, indicating a significant difference in the dynamics between the transmembrane and soluble domains of the protein (Fig. 2 *F*). Typical behavior of CP buildup rate was observed for the peak at 93.5 ppm—intensity buildup during a short CP contact time is dominated by the ^{1}H-^{15}N polarization transfer due to N-H dipolar coupling and a loss of magnetization after saturation due to $T_{1\rho}$. Conversely, the peak at 128.4 ppm builds up slowly and does not decay with the increasing CP contact time, indicating the effect of a smaller N-H dipolar coupling due to faster dynamics in the soluble domain of the protein.

Fitting the CP buildup curves using Eq. 1 provided an estimation of proton spin-lattice relaxation time in the rotating frame ($T_{1\rho}{}^{H}$) and the polarization transfer time-constant (T_{NH}) (26) for the transmembrane domain (at 93.5 ppm), which are 1.61 ± 0.36 ms and 0.26 ± 0.05 ms, respectively. These two relaxation parameters reflect submillisecond timescale motions of the corresponding residues, which may include rotational diffusion of the whole helix and fluctuation of the helical director axis, and thus can be used to indicate changes in the dynamics of the transmembrane domain upon changes in the lipid membrane composition or interaction with other proteins. This is demonstrated here by using a lipid composition of DLPC/DHPC. The removal of cholesterol from bicelles increases the dynamics of the transmembrane domain as reflected by a longer $T_{1\rho}{}^{H}$ value of 2.08 ± 0.57 ms at 93.5 ppm (data not shown). This is most likely attributed to the effect of cholesterol that rigidifies the lipid membrane, which in turn affects the rotational diffusion of the transmembrane helix.

$$I(t) = \frac{I(0)}{T_{NH}}\left(e^{-\frac{t}{T_{1\rho}^{H}}} - e^{-\frac{t}{T_{NH}}}\right)\left(\frac{1}{T_{NH}} - \frac{1}{T_{1\rho}^{H}}\right)^{-1} \quad (1)$$

Two-dimensional SLF experiment and simulation of helical wheels

Two-dimensional SLF spectra, which correlate ^{15}N chemical shift with ^{1}H-^{15}N dipolar coupling, were obtained to characterize the structure and further investigate the dynamics of the transmembrane domain of the protein (Fig. 4). In the frequency region assigned to the transmembrane domain (70–100 ppm), a discernible circular wheel-like pattern of resonances was observed, which is unique for proteins with an α-helical conformation. To our knowledge, this is the first experimental evidence of an α-helical secondary structure for the transmembrane domain of CYPOR, agreeing with some of the postulations in the literature (11–13). In the region assigned to the soluble domain (100–140 ppm), we also observed resonances with small dipolar coupling values, suggesting a weak alignment of the soluble domain in the bicelle environment.

To further characterize the orientation and dynamics of the transmembrane helix, we performed a spectral simulation to fit the observed resonances into a helical-wheel pattern. Simulations demonstrate the sensitivity of the wheel pattern to the helix tilt angle (with respect to membrane normal) and the order parameter as shown in Fig. 5, *A–C*. The best-fit helical wheel (Fig. 5, *D* and *E*) indicates an average tilt angle of 13° ± 2° (27) and the overall order parameter *S* of 0.80. The order parameter reflects a collection of motions that the α-helix exhibits in the lipid bilayer, ranging from rotational diffusion to fluctuation of the helical director axis, the schematic of which is shown in Fig. 5 *F*. Similar tilt angle and order parameter have also been observed for the transmembrane domain of cytochrome b_5 (21,25). As shown in Fig. 5, *D* and *E*, no single helical wheel can fit all the resonances in the circular pattern, implying a nonideality of the transmembrane helix.

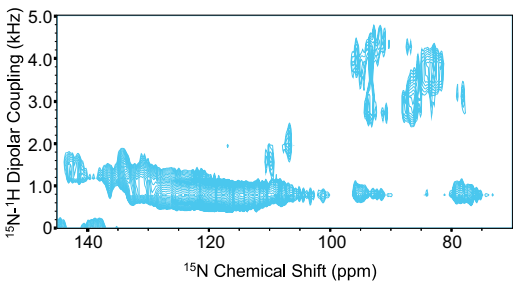

FIGURE 4 Two-dimensional ^{15}N separated-local-field NMR spectrum of a uniformly ^{15}N-labeled MFBD incorporated in magnetically aligned DLPC/DHPC/cholesterol bicelles. The spectrum was collected with a 0.5-ms CP contact time and 25 kHz SPINAL16 decoupling. To see this figure in color, go online.

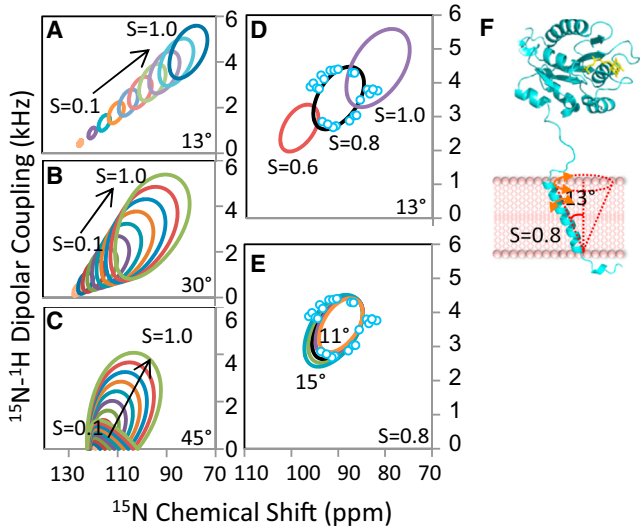

FIGURE 5 (*A–C*) Simulated helical wheels showing the sensitivity of the wheel pattern to the indicated tilt angle of the helix. (*D* and *E*) Fitting of the observed resonances in two-dimensional SLF spectra (*blue circles*) with different tilt angles and order parameters (*S*). The tilt angle used in panel *D* is 13° with order parameters S of 0.6 (*red*), 0.8 (*black*), and 1.0 (*purple*). The order parameter used in panel *E* is 0.8 with varied tilt angles: 11° (*orange*), 12° (*purple*), 13° (*black*), 14° (*green*), and 15° (*blue*). The best-fitting wheel indicates an average helical tilt angle of 13° and an order parameter S of 0.8 (*F*) for the transmembrane helix of the MFBD protein embedded in magnetically aligned DLPC/DHPC/cholesterol bicelles. To see this figure in color, go online.

Additional experiments using selectively labeled MFBD will be carried out to assign the spectra and to study MFBD-cyt P450 interaction.

DISCUSSION

Secondary structure of the transmembrane domain of CYPOR in a lipid environment

Previous studies have reported the importance of the transmembrane domain of CYPOR in complex formation with cyt P450 and substrate metabolism mediated by cyt P450 (8–10,28–30). It is generally believed that the N-terminal hydrophobic segment of CYPOR serves as a membrane anchor and aids in the interaction with cyt P450 and electron transfer between CYPOR and cyt P450 (6). However, the mechanism on how the transmembrane domain affects cyt P450/CYPOR interaction and substrate catalysis remains under debate (8), and the experimental evidences to unveil the mist are highly deficient. To better understand the physiological function of the transmembrane domain of CYPOR, we investigated its structure and dynamics in a lipid membrane environment using static solid-state NMR experiments.

An early study predicted the transmembrane domain of CYPOR to contain a β-sheet structure and possibly adopt a U-shaped structure in the membrane (10), whereas in

recent years it has been presumed to contain an α-helical conformation spanning the lipid bilayer (11–13). Results reported in this study present, to our knowledge, the first experimental evidence of an α-helical secondary structure for the transmembrane domain, which is in agreement with previous hypotheses (11–13). The overall order parameter of the transmembrane domain coincides with those observed in the membrane-spanning transmembrane helices in the literature, further supporting that the transmembrane helix of CYPOR spans the lipid bilayer (31–33). The tilt angle of the transmembrane helix relative to the lipid bilayer normal can be determined from the experimentally measured N-H dipolar couplings, and it can be affected by the hydrophobic mismatch between the length of the transmembrane helix and the hydrophobic thickness of the lipid bilayer (32). The experimentally determined tilt angle of 13° for the transmembrane helix of CYPOR is comparable with those reported for cytochrome b_5 (13°) and cytochrome P450 (17°), revealing the geometrical similarity in the transmembrane domains of these electron transfer partners. The interplay between the transmembrane domains of these proteins and their role in affecting electron transfer and complex formation is currently under investigation in our laboratory.

Distinct dynamics of the soluble and transmembrane domains of CYPOR

Motions and structural dynamics are essential for the physiological function of membrane proteins. To gain insight into the role of the transmembrane domain of CYPOR in protein-protein interactions, we first experimentally determined the dynamic behavior of MFBD. In a series of CP experiments on magnetically aligned bicelles containing ^{15}N-labeled MFBD (Fig. 2), we observed distinct difference between the timescales of dynamics for the soluble and transmembrane domains. Because the magnetically aligned bicelles do not tumble rapidly, the rate of magnetization transfer from ^{1}H to ^{15}N in a CP experiment (also known as the CP buildup rate) is dominated by the dipolar interactions that are very sensitive to submillisecond molecular motions. Evidently, faster CP buildup and decay rates of the transmembrane domain signals (Fig. 2 *F*) indicate restrained motions of the transmembrane domain compared to the residues in the soluble domain of the MFBD protein. Further analysis of the CP process also resulted in an estimation of $T_{1\rho}{}^{H}$ and T_{NH} values, which qualitatively reflect the mobility of the corresponding resonances.

In the two-dimensional SLF spectrum of magnetically aligned bicelles containing ^{15}N-labeled-MFBD (shown in Fig. 4), the difference between the mobility of the two domains is clearly indicated by the magnitudes of the N-H dipolar couplings. The heteronuclear N-H dipolar coupling reports on the amplitude of local motions occurring on a timescale faster than the inverse of this interaction. The average N-H dipolar couplings observed for the transmembrane domain are approximately three times larger than those observed for the soluble domain of MFBD, implying that the soluble domain undergoes motions of larger amplitude in the submillisecond timescale. These results are in excellent agreement with the result obtained from the one-dimensional CP experiments.

The distinct dynamic characteristics of the two domains are highly correlated with their functions. The soluble FMN binding domain is suggested to be able to diffuse rapidly in the cytosol for a fast association and dissociation with cyt P450 to occur and to maximize the turnover rate of electron transfer. On the other hand, the small dipolar couplings of ~1 kHz (or lesser) observed for the soluble domain (Fig. 4) imply a weak alignment of this domain or a transient interaction with the lipid bilayer instead of isotropic tumbling/diffusion like a globular protein. This may be attributed to the membrane-anchoring effect of the transmembrane domain, which may constrain the diffusion of the soluble domain to the proximity of the membrane surface by positioning the protein suitably for an effective interaction with cyt P450. Besides serving as a membrane anchor, the transmembrane domain of CYPOR might also be involved in hetero-recognition with the transmembrane domain of cyt P450. The structural and dynamic studies presented in this study would be valuable to test this hypothesis in further investigations. In a lipid bilayer, the motions of a single α-helix can be visualized as rotational diffusion around the membrane normal and fluctuation of the helix tilt (21). The amplitude of these motions collectively influences the magnitude of observed NMR parameters, in particular the chemical shift anisotropy and dipolar coupling (34,35). By measuring the dipolar coupling values and determining the order parameter, we can monitor the changes in the dynamics of the transmembrane domain upon changes in the lipid environment or in the protein-protein interactions.

CONCLUSION

In this study, we have reported a solid-state NMR investigation of the structure and dynamics of the FMN binding domain of CYPOR, including the transmembrane helix and the linker region, in a native-like membrane environment using magnetically aligned bicelles. We have provided what is, to our knowledge, the first experimental evidence of an α-helical conformation for the rigid transmembrane anchor of CYPOR. The measured N-H dipolar couplings and the CP buildup rates suggest the difference in the timescales of dynamics between the soluble and transmembrane domains: the transmembrane domain undergoes a slow motion (in the millisecond timescale) whereas the soluble domain undergoes a fast motion (in the microsecond timescale). The successful implementation of a combination of one-dimensional CP and two-dimensional SLF experiments on

magnetically aligned bicelles provides a simple method for further investigations on the structural and dynamic properties of the full-length CYPOR and its interaction with other membrane proteins in a membrane environment.

SUPPORTING MATERIAL

Amino Acid Sequence of Membrane-Bound FMN Binding Domain (MFBD) of Rat CYPOR and reference (36) is available at http://www.biophysj.org/biophysj/supplemental/S0006-3495(14)00403-2.

We thank Dr. Patrick Walsh and Samuel Kotler for their critical reading of the manuscript.

This research was supported by the National Institutes of Health under grants No. GM084018 and No. GM095640 to A.R. and partly by grant No. GM094209 and a VA Merit Review grant to L.W. We acknowledge the use of the NMR facility at the National High Magnetic Field Laboratory supported by the National Science Foundation and by the State of Florida through Cooperative Agreement No. DMR-0084173.

REFERENCES

1. Shen, A. L., K. A. O'Leary, and C. B. Kasper. 2002. Association of multiple developmental defects and embryonic lethality with loss of microsomal NADPH-cytochrome P450 oxidoreductase. *J. Biol. Chem.* 277:6536–6541.
2. Williams, Jr., C. H., and H. Kamin. 1962. Microsomal triphosphopyridine nucleotide-cytochrome *c* reductase of liver. *J. Biol. Chem.* 237:587–595.
3. Enoch, H. G., and P. Strittmatter. 1979. Cytochrome b_5 reduction by NADPH-cytochrome P-450 reductase. *J. Biol. Chem.* 254:8976–8981.
4. Schacter, B. A., E. B. Nelson, …, B. S. Masters. 1972. Immunochemical evidence for an association of heme oxygenase with the microsomal electron transport system. *J. Biol. Chem.* 247:3601–3607.
5. Bachur, N. R., S. L. Gordon, …, H. Kon. 1979. NADPH cytochrome P-450 reductase activation of quinone anticancer agents to free radicals. *Proc. Natl. Acad. Sci. USA.* 76:954–957.
6. Wang, M., D. L. Roberts, …, J. J. Kim. 1997. Three-dimensional structure of NADPH-cytochrome P450 reductase: prototype for FMN- and FAD-containing enzymes. *Proc. Natl. Acad. Sci. USA.* 94:8411–8416.
7. Xia, C., S. P. Panda, …, J. J. Kim. 2011. Structural basis for human NADPH-cytochrome P450 oxidoreductase deficiency. *Proc. Natl. Acad. Sci. USA.* 108:13486–13491.
8. Gideon, D. A., R. Kumari, …, K. M. Manoj. 2012. What is the functional role of N-terminal transmembrane helices in the metabolism mediated by liver microsomal cytochrome P450 and its reductase? *Cell Biochem. Biophys.* 63:35–45.
9. Gum, J. R., and H. W. Strobel. 1981. Isolation of the membrane-binding peptide of NADPH-cytochrome P-450 reductase. Characterization of the peptide and its role in the interaction of reductase with cytochrome P-450. *J. Biol. Chem.* 256:7478–7486.
10. Black, S. D., and M. J. Coon. 1982. Structural features of liver microsomal NADPH-cytochrome P-450 reductase. Hydrophobic domain, hydrophilic domain, and connecting region. *J. Biol. Chem.* 257:5929–5938.
11. Sündermann, A., and C. Oostenbrink. 2013. Molecular dynamics simulations give insight into the conformational change, complex formation, and electron transfer pathway for cytochrome P450 reductase. *Protein Sci.* 22:1183–1195.
12. Im, S. C., and L. Waskell. 2011. The interaction of microsomal cytochrome P450 2B4 with its redox partners, cytochrome P450 reductase and cytochrome b_5. *Arch. Biochem. Biophys.* 507:144–153.
13. Dürr, U. H., L. Waskell, and A. Ramamoorthy. 2007. The cytochromes P450 and b_5 and their reductases—promising targets for structural studies by advanced solid-state NMR spectroscopy. *Biochim. Biophys. Acta.* 1768:3235–3259.
14. Bridges, A., L. Gruenke, …, L. Waskell. 1998. Identification of the binding site on cytochrome P450 2B4 for cytochrome b_5 and cytochrome P450 reductase. *J. Biol. Chem.* 273:17036–17049.
15. Gutierrez, A., L. Y. Lian, …, G. C. Roberts. 2001. Stopped-flow kinetic studies of flavin reduction in human cytochrome P450 reductase and its component domains. *Biochemistry.* 40:1964–1975.
16. Yamamoto, K., M. Gildenberg, …, A. Ramamoorthy. 2013. Probing the transmembrane structure and topology of microsomal cytochrome-p450 by solid-state NMR on temperature-resistant bicelles. *Sci. Rep.* 3:2556.
17. Morris, G. A., and R. Freeman. 1979. Enhancement of nuclear magnetic-resonance signals by polarization transfer. *J. Am. Chem. Soc.* 101:760–762.
18. Ramamoorthy, A., and N. Chandrakumar. 1992. Comparison of the coherence-transfer efficiencies of laboratory-frame and rotating-frame experiments. *J. Magn. Reson.* 100:60–68.
19. Metz, G., X. L. Wu, and S. O. Smith. 1994. Ramped-amplitude cross-polarization in magic-angle-spinning NMR. *J. Magn. Reson. A.* 110:219–227.
20. Gor'kov, P. L., E. Y. Chekmenev, …, W. W. Brey. 2007. Using low-E resonators to reduce RF heating in biological samples for static solid-state NMR up to 900 MHz. *J. Magn. Reson.* 185:77–93.
21. Soong, R., P. E. Smith, …, A. Ramamoorthy. 2010. Proton-evolved local-field solid-state NMR studies of cytochrome b_5 embedded in bicelles, revealing both structural and dynamical information. *J. Am. Chem. Soc.* 132:5779–5788.
22. Dürr, U. H., M. Gildenberg, and A. Ramamoorthy. 2012. The magic of bicelles lights up membrane protein structure. *Chem. Rev.* 112:6054–6074.
23. Yamamoto, K., P. Pearcy, and A. Ramamoorthy. 2014. Bicelles exhibiting magnetic alignment for a broader range of temperatures: a solid-state NMR study. *Langmuir.* 30:1622–1629.
24. Dürr, U. H., K. Yamamoto, …, A. Ramamoorthy. 2007. Solid-state NMR reveals structural and dynamical properties of a membrane-anchored electron-carrier protein, cytochrome b_5. *J. Am. Chem. Soc.* 129:6670–6671.
25. Yamamoto, K., U. H. Dürr, …, A. Ramamoorthy. 2013. Dynamic interaction between membrane-bound full-length cytochrome P450 and cytochrome b_5 observed by solid-state NMR spectroscopy. *Sci. Rep.* 3:2538.
26. Kawamura, I., M. Ohmine, …, A. Naito. 2007. Dynamic aspects of extracellular loop region as a proton release pathway of bacteriorhodopsin studied by relaxation time measurements by solid state NMR. *Biochim. Biophys. Acta.* 1768:3090–3097.
27. Salnikov, E., P. Bertani, …, B. Bechinger. 2009. Analysis of the amide ^{15}N chemical shift tensor of the Cα tetrasubstituted constituent of membrane-active peptaibols, the α-aminoisobutyric acid residue, compared to those of di- and tri-substituted proteinogenic amino acid residues. *J. Biomol. NMR.* 45:373–387.
28. Müller-Enoch, D., and H. Gruler. 2000. Complexation of membrane-bound enzyme systems. *Z. Naturforsch., C, J. Biosci.* 55:747–752.
29. Estabrook, R. W., M. R. Franklin, …, A. G. Hildebrandt. 1971. Biochemical and genetic factors influencing drug metabolism. Influence of hepatic microsomal mixed function oxidation reactions on cellular metabolic control. *Metabolism.* 20:187–199.
30. Black, S. D., J. S. French, …, M. J. Coon. 1979. Role of a hydrophobic polypeptide in the N-terminal region of NADPH-cytochrome P-450 reductase in complex formation with P-450LM. *Biochem. Biophys. Res. Commun.* 91:1528–1535.
31. De Angelis, A. A., S. C. Howell, …, S. J. Opella. 2006. Structure determination of a membrane protein with two *trans*-membrane helices in

aligned phospholipid bicelles by solid-state NMR spectroscopy. *J. Am. Chem. Soc.* 128:12256–12267.

32. Park, S. H., A. A. De Angelis, …, S. J. Opella. 2006. Three-dimensional structure of the transmembrane domain of Vpu from HIV-1 in aligned phospholipid bicelles. *Biophys. J.* 91:3032–3042.
33. Müller, S. D., A. A. De Angelis, …, A. S. Ulrich. 2007. Structural characterization of the pore forming protein TatAd of the twin-arginine translocase in membranes by solid-state ^{15}N-NMR. *Biochim. Biophys. Acta.* 1768:3071–3079.
34. Esteban-Martín, S., E. Strandberg, …, J. Salgado. 2009. Influence of whole-body dynamics on ^{15}N PISEMA NMR spectra of membrane proteins: a theoretical analysis. *Biophys. J.* 96:3233–3241.
35. Park, S. H., A. A. Mrse, …, S. J. Opella. 2006. Rotational diffusion of membrane proteins in aligned phospholipid bilayers by solid-state NMR spectroscopy. *J. Magn. Reson.* 178:162–165.
36. Krogh, A., B. Larsson, …, E. L. Sonnhammer. 2001. Predicting transmembrane protein topology with a hidden Markov model: application to complete genomes. *J. Mol. Biol.* 305:567–580.

Probing the transmembrane structure and dynamics of microsomal cytochrome P450 reductase by solid-state NMR

Rui Huang*, Kazutoshi Yamamoto[*], Meng Zhang[*], Nataliya Popovych[*], Ivan Hung[‡], Sang-choul Im[†], Zhehong Gan[‡], Lucy Waskell[†] and Ayyalusamy Ramamoorthy[*]

*Biophysics and Department of Chemistry, University of Michigan, Ann Arbor, MI, 48109-1055; †Department of Anesthesiology, University of Michigan, and VA Medical Center, Ann Arbor, MI 48105; ‡National High Magnetic Field Lab, Tallahassee, FL, 32310-3708.

Supporting Material

Amino acid sequence of membrane-bound FMN binding domain (MFBD) of rat CPR. The transmembrane domain is underlined according to TMHMM prediction (1).

10	20	30	40	50	60
MGDSHEDTSA	TMPEAVAEEV	SLFSTTDMVL	FSLIVGVLTY	WFIFRKKKEE	IPEFSKIQTT
70	80	90	100	110	120
APPVKESSFV	EKMKKTGRNI	IVFYGSQTGT	AEEFANRLSK	DAHRYGMRGM	SADPEEYDLA
130	140	150	160	170	180
DLSSLPEIDK	SLVVFCMATY	GEGDPTDNAQ	DFYDWLQETD	VDLTGVKFAV	FGLGNKTYEH
190	200	210	220	230	
FNAMGKYVDQ	RLEQLGAQRI	FELGLGDDDG	NLEEDFITWR	EQFWPAVCEF	FGVEATGEE

References

1. Krogh, A., B. Larsson, G. von Heijne, and E. L. Sonnhammer. 2001. Predicting transmembrane protein topology with a hidden Markov model: application to complete genomes. J Mol Biol 305:567-580.